Controlling the Thermal Polymerization Process of Hybrid Organic−Inorganic Films Synthesized from 3-Methacryloxypropyltrimethoxysilane and 3-Aminopropyltriethoxysilane

Plinio Innocenzi*

Materials Science and Nanotechnology Laboratory, Dipartimento di Architettura e Pianificazione, Università di Sassari, Palazzo Pou Salid, Piazza Duomo, 07041 Alghero, Sassari, Italy

Giovanna Brusatin

Settore Materiali, Dipartimento di Ingegneria Meccanica, Università di Padova, via Marzolo 9, 35131, Padova, Italy

Silvia Licoccia and Maria Luisa Di Vona

Dipartimento di Scienze e Tecnologie Chimiche, Universita' di Roma Tor Vergata, via della Ricerca Scientifica 1, 00133 Roma, Italy

Florence Babonneau

Chimie de la Matière Condensée, Université Paris, 6 T54 E5, 4 place Jussieu, 75252 Paris Cedex 05, France

Bruno Alonso

CRMHT, CNRS UPR 4212, 1D av. de la Recherche Scientifique, 45071 Orléans Cedex 2, France

Received May 7, 2003. Revised Manuscript Received September 15, 2003

An important step in the synthesis of hybrid materials is the control of organic chains formation when the organically modified alkoxides are bearing polymerizable groups, such as acrylate or epoxy. Control of the process can be achieved through a deep understanding of the correlation between the synthesis parameters and the final structure. In this paper we have used 3-methacryloxypropyltrimethoxysilane (MPTMS) co-hydrolyzed with tetraethyl orthosilicate (TEOS) using 3-aminopropyltriethoxysilane (APTS) as basic catalyst and network modifier of the structure. The acrylate function in MPTMS has been thermally polymerized and the process has been tuned, with the purpose to reach the highest polymerization efficiency, by controlling the synthesis parameters. The synthesis has been followed in solution by ^{13}C and ^{29}Si nuclear magnetic resonance (NMR) spectroscopy, and the structural changes in the films have been studied by Fourier transform infrared spectroscopy (FTIR) as a function of the thermal treatment. Multinuclear solid state NMR spectroscopy on related bulk materials has provided supplementary information on the hybrid network formation. As-deposited films are not fully condensed but a very large conversion of the C═C double bonds (up to 98% of polymerization degree) is achieved during thermal curing by the simultaneous inorganic polycondensation and organic polymerization.

Introduction

Hybrid organic−inorganic materials are currently used for a large variety of functional purposes, one of the most diffused commercial applications being their use as coating films.[1] The definition of hybrid materials is, however, quite wide, and several attempts have been made to achieve a classification of these new materials on the basis of their structural properties.[2] The complete understanding of hybrids structure is still far from being exhaustive, with the intrinsic hybrid nature shadowing the definition and comprehension of several properties. Following the classification by Sanchez et al.,[2] class II of hybrids is the one that exhibits a true interconnection, via covalent bonding, between the organic and inorganic

* To whom correspondence should be addressed. E-mail: plinio.innocenzi@unipd.it, plinio@uniss.it.

(1) (a) Nass, R.; Arpac, E.; Glaubitt, W.; Schmidt, H. *J. Non-Cryst. Solids* **1990**, *121*, 370. (b) Popall, M.; Kappel, J.; Pilz, M.; Schulz, J.; Feyder, G. *J. Sol-Gel Sci. Technol.* **1994**, *2*, 157. (c) Schmidt, H. *J. Non-Cryst. Solids* **1994**, *178*, 302.

(2) Sanchez, C.; Ribot, F. *New J. Chem.* **1994**, *18*, 1007.

10.1021/cm0343305 CCC: $25.00
Published on Web 11/15/2003

components. Interpenetrated organic and inorganic networks may be present in hybrids of class I, however, the two networks remain as two separated domains connected only via mechanical entanglements or secondary bonding. Guest−host systems, in which organic molecules are incorporated within an oxide matrix, fall within this class. In class II the organic groups are directly connected to the inorganic network and their role can be that of a network modifier, for instance, alkali ions in silica. A peculiar group of the class II hybrids is characterized, instead, by the presence of polymerizable organic groups, such as vinylic,[3] acrylate,[4] or epoxy.[5] They can be partially or completely polymerized directly in the sol using proper synthetic conditions: a common case is that of the epoxy containing alkoxides.[6] Alternatively, photo or thermal curing of the materials is used to achieve polymerization.[7] These materials develop, therefore, two different interconnected networks: an inorganic one and an organic one whose extension and configuration are mutually dependent.

Control of the organic polymerization is a crucial step in the synthesis of these hybrid materials. In fact, most of the final properties, such as mechanical and optical characteristics, are affected by the length of the chains, the degree of interconnection between the organic polymers, and the homogeneity of the material. The very fine control of the polymerization is, however, a more difficult task than in pure organic polymers, because the two covalently linked organic and inorganic networks are formed at different rates and yields. In "conventional" sol−gel processes, the inorganic network is generated through hydrolysis and condensation reactions of molecular precursors (ions, alkoxides, chlorides, etc.) and usually reaches a much larger extension than the polymeric network, so that the growth of the organic chains is strongly hindered. This has been described in the case of materials synthesized from 3-glycidoxypropyltrimethoxysilane,[8] but this behavior can be extended to other polymerizable functionalities, even if a case-by-case study is necessary for the exact tuning of the material structure.

Among these materials an interesting group is represented by hybrids synthesized from organically modified alkoxides bearing amine functionalities. The interest in these materials is justified by several applications, such as oxygen barrier layers,[3] optical waveguides,[9] and host matrix for photonic organic dyes that are degraded in an acidic environment, like the zwitterionic molecules.[10] These alkoxides are organic modifiers of the network but are also basic catalysts for the inorganic condensation. They can be cohydrolyzed with different polymerizable organically modified alkoxides to give a final material with controlled properties.

Table 1. Gelation Times of the Precursor Sols prepared using Different Alkoxides Molar Ratios[a]

sample	chemical composition (molar ratio) MPTMS	TEOS	APTS	H_2O	gelation time (h)
MTA1-0.05-2	1.00	1	0.10	4.0	5.3
MTA1-0.07-2	1.00	1	0.14	4.0	4.0
MTA1-0.1-2	1.00	1	0.20	4.0	2.3
MTA2.33-0.05-2	2.33	1	0.17	6.7	20.0
MTA2.33-0.07-2	2.33	1	0.23	6.7	4.0
MTA2.33-0.1-2	2.33	1	0.33	6.7	2.0

[a] The data are referred to sols synthesized using a $H_2O/SiO_2 = 2$ molar ratio.

In this paper we have used 3-aminopropyltriethoxysilane (APTS) in combination with 3-methacryloxypropyltrimethoxysilane (MPTMS), and tetraethyl orthosilicate (TEOS) in a simple synthetic process, with the purpose of fabricating an optically transparent film in the visible range where a large degree of organic polymerization is achieved through the control of the processing conditions. The synthesis has been studied by liquid-state nuclear magnetic resonance (NMR); Fourier transformed infrared spectroscopy (FTIR) and multinuclear solid-state NMR have been used to study the effect of thermal polymerization on the hybrid films and related bulk materials.

Experimental Section

Materials. The precursor sol was synthesized employing tetraethyl orthosilicate (TEOS), 3-methacryloxypropyltrimethoxysilane (MPTMS), and 3-aminopropyltriethoxysilane (APTS) as precursors. They were all purchased from Aldrich and used without further purification. Ethanol (EtOH) (Prolabo) was employed as solvent, and bidistilled water was used for hydrolysis.

Synthesis of the Sol. MPTMS and TEOS were first mixed in ethanol, immediately afterward water was added, and the sol was stirred in a closed vessel at room temperature for 15 min followed by the addition of APTS. After 5 min of stirring the sol was used to prepare the films.

The molar ratios were as follows: MPTMS/TEOS, 2.33 or 1; APTS/(MPTMS + TEOS), 0.05, 0.07, or 1; H_2O/(MPTMS + TEOS), 2 or 3. The solvent was added in an amount to reach a 100 gL^{-1} concentration of oxide in the sol. Samples have been labeled with three different numbers to indicate the different ratios employed; for instance MTA2.33-0.05-2 for a sample obtained by a sol synthesized using the molar ratios MPTMS/TEOS = 2.33, APTS/(MPTMS + TEOS) = 0.05, and H_2O/(MPTMS + TEOS) = 2. Samples ($H_2O/SiO_2 = 2$) with their compositions (in molar ratios) and gelation times are listed in Table 1.

NMR Characterization. ^{13}C and ^{29}Si liquid NMR spectra were recorded at the probe temperature (298 K) with a Bruker Avance 400 spectrometer operating at 100.6 and 79.49 MHz, respectively. ^{29}Si MAS NMR spectra were recorded on a MSL400 Bruker spectrometer with a 7-mm CP MAS probe, using 90° pulse duration (6.5 μs) and 100 s recycle delays. The spinning rate was 4 kHz. $^{13}C\{^1H\}$ solid-state NMR spectra were acquired on a Bruker DSX 400 spectrometer ($^1H \equiv 400.13$ MHz) under ^1H decoupling. A double resonance ^1H-X probe using 4-mm ZrO_2 rotors span at a magic angle spinning (MAS)

(3) Hoffmann, M.; Amberg-Schwab, S. *MRS Symp. Proc.* **1998**, *519*, 309.

(4) Delattre, L.; Dupuy, C.; Babonneau, F. In *Proceedings of the First European Workshop on Hybrid Materials*; Sanchez, C., Ed.; Bierville, France, 1993; p 185.

(5) Schmidt, H. *MRS Symp. Proc.* **1984**, *32*, 327. (2) Schmidt, H. *J. Non-Cryst. Solids* **1994**, *178*, 302. (3) Schmidt, H. *J. Sol-Gel Sci. Technol.* **199**7, *8*, 557.

(6) (1) Innocenzi, P.; Brusatin, G.; Guglielmi, M.; Bertani, R. *Chem. Mater.* **1999**, *11*, 1672. (2) Innocenzi, P.; Sassi, A.; Brusatin, G.; Guglielmi, M.; Favretto, D.; Bertani, R.; Venzo, A.; Babonneau, F. *Chem. Mater.* **2001**, *13*, 3635.

(7) (a) Soppera, O.; Croutxè-Barghorn, C.; Lougnot, D. J. *New J. Chem.* **2001**, *25*, 1006. (b) Medda, S. K.; Kundu, D.; De, G. *J. Non-Cryst. Solids* **2003**, *318*, 149.

(8) Innocenzi, P.; Brusatin, G.; Babonneau, F. *Chem. Mater.* **2000**, *12*, 3726.

(9) Nassar, E. J.; Goncalves, R. R.; Ferrari, M.; Messadeq, Y.; Ribeiro, S. J. L. *J. Alloys Compd.* **2002**, *344*, 221.

(10) Innocenzi, P.; Miorin, E.; Brusatin, G.; Abbotto, A.; Beverina, L.; Pagani, G.; Casalboni, M.; Pizzoferrato, R.; Sarcinelli, F. *Chem. Mater.* **2002**, *14*, 3758.

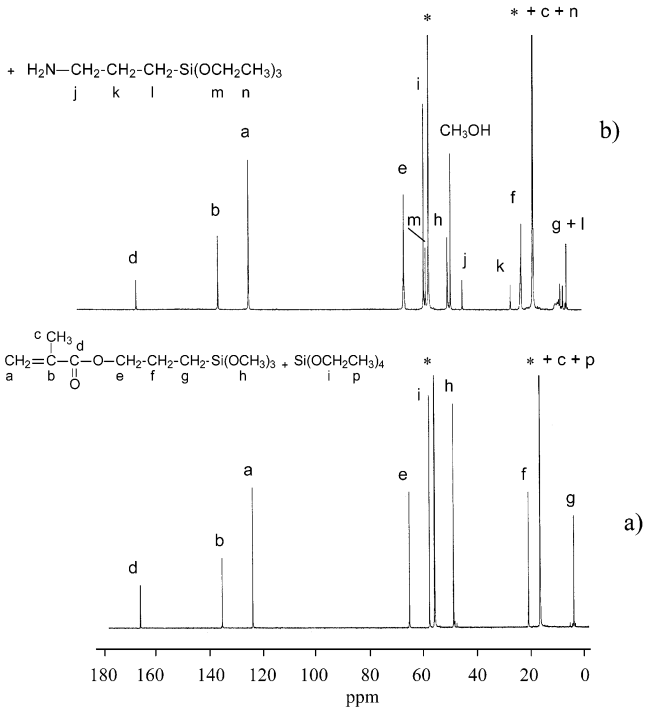

Figure 1. ^{13}C NMR spectra of the precursor sols MTA2.33-0.07-2. An asterisk marks the solvent signals; (a) MPTMS + TEOS + H_2O. (b) (a) + APTS.

rate of 11 kHz was employed. The radio frequency field strengths for ^{1}H and ^{13}C pulses were 50 kHz. Optimal conditions for $^{13}C\{^{1}H\}$ cross-polarization (CP) spectra were a number of 512 scans, a recycle delay of 5 s, and a contact time of 2 ms. Chemical shift referencing is relative to external TMS for ^{13}C, ^{1}H, and ^{29}Si NMR spectra.

Materials Preparation. Films were deposited via dip-coating on pre-cleaned soda−lime glass substrates and on silicon wafers. The samples were thermally cured in air at different temperatures (60, 80, 100, 120, 140, 180, 220, and 250 °C) for 30 min.

Powders were prepared by pouring the sol into glassware and drying it at 60 °C. The dried gel was milled to obtain a fine powder. These powders were used for multinuclear solid-state NMR spectroscopy.

FTIR Characterization. Infrared absorption spectra in the range 4500−400 cm^{-1} were recorded by Fourier transform infrared spectroscopy (FTIR) (Perkin-Elmer 2000), with a resolution of ±1 cm^{-1}, 256 scans, on films deposited on silicon wafers. A Gaussian peak fitting procedure has been applied to the FTIR spectra (Microcal Origin Software), the quality of the fitting was evaluated on the basis of the χ^2-values (in the order of 10^{-6}) and correlation coefficient values ≥ 0.998.

Results and Discussion

Study of the Reactions in the Precursor Sol. Sample MTA2.33-0.07-2 was chosen as a representative example to study the hydrolysis and condensation process by means of ^{13}C and ^{29}Si liquid-state NMR.

The reaction was followed during the two main steps of the synthesis: before and after the addition of APTS. Figure 1a shows the ^{13}C NMR spectrum of the ethanolic solution containing MPTMS and TEOS after the addition of water, the assignments are reported in the Figure 1a.[8] The spectrum appears to be the sum of those of the pure species. This is confirmed by the ^{29}Si NMR spectrum of the same solution: only the peaks due to MPTMS ($\delta = -42.8$ ppm) and TEOS ($\delta = -82.4$ ppm) are observed, (Figure 2a).

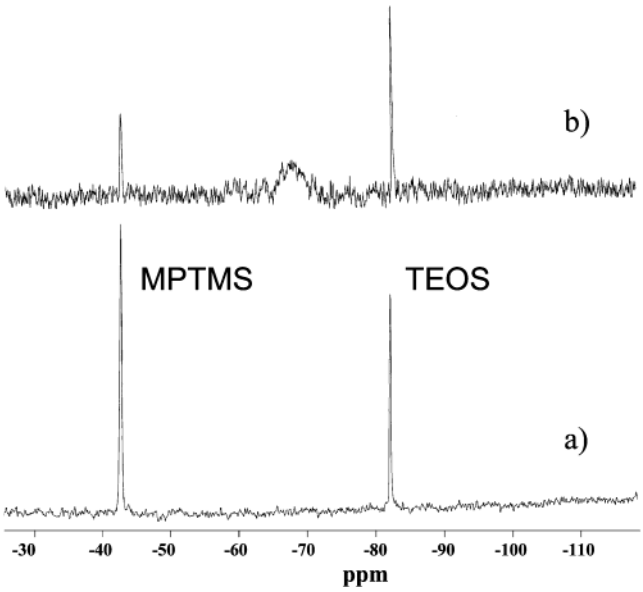

Figure 2. ^{29}Si NMR spectrum of the sol MTA2.33-0.07-2. (a) MPTMS + TEOS + H_2O. (b) (a) + APTS

The ^{13}C spectrum of the mixture after the addition of APTS is shown in Figure 1b. The lack of variation observed for the $-OCH_2$ groups in TEOS (labeled i) indicates that it is largely unreacted. In contrast, reactions involving hydrolysis of MPTMS are evidenced by the changes observed for the resonance peaks due to the propyl chain: resonances f and g appear broader, while several signals are now present between 5 and 10 ppm where the peak due to the amine CH_2 (l) is also present. The presence of a new resonance at 49.3 ppm due to methyl alcohol is also observed. As these alcohol molecules cannot be the result of trans-alcoholysis reaction (vide infra), they indicate the hydrolysis of methoxy functions.

No shifts of the peaks due to the quaternary and olefinic carbons are observed and this indicates that no reaction involving the acrylic double bond occurs.

The ^{29}Si NMR spectrum of the mixture is shown in Figure 2b. Again, this confirms that TEOS is substantially unreacted because no peaks appear at $\delta < -82.4$ ppm where resonances due to condensation of polysiloxanes are expected.[9] MPTMS is also present in solution but in much lower amount, whereas APTS has totally reacted since no resonance peak is observed at −44.7 ppm.[10] Indeed, the main feature of the spectrum is the broad signal centered at −67.6 ppm, corresponding to T_3 unit,[9] which can be assigned to condensation products of $R-CH_2-Si-(OR)_3$ species, i.e., MPTMS and APTS. The presence of only T_0 and T_3 units is in agreement with a monomer-cluster condensation mechanism, which is expected under basic conditions.

The spectrum allows elimination of the possibility that the methyl alcohol formation detected in the ^{13}C NMR spectrum could be due to ligand exchange reactions between Si−OMe groups of MPTMS and EtOH used as solvent under basic conditions. No new sharp peak is observed at $\delta < -42.6$ ppm where $R-Si(OMe)_x(OEt)_{4-x}$ species would appear.[9]

This NMR study suggests that APTS acts as a basic catalyst for the condensation of MPTMS that undergoes hydrolysis followed by self-condensation or condensation with APTS.

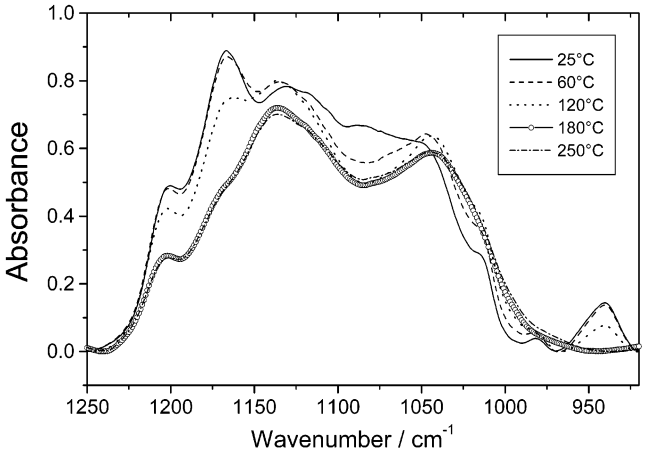

Figure 3. FTIR absorption spectra in the range 1250−870 cm^{-1} of MTA2.33-0.05-2 films thermally cured at 25 (as-deposited), 60, 120, 180, and 250 °C.

FTIR Analysis of the Films. It is known that the preferential evaporation of ethanol that occurs during dip-coating strongly favors the condensation between alkoxy groups.[11] This process creates, in fact, a water-rich film where the hydrolysis and condensation reactions occur simultaneously with the drying stage to yield, in a complex and rapid way, the final film structure.

Figure 3 shows the FTIR absorption spectra of MTA2.33-0.07-2 films in the range 1250−870 cm^{-1}. Bands due to the vibrations of unreacted TEOS and MPTMS are observed at 1168 cm^{-1} ($\delta(CH_3)$), 1028 cm^{-1} ($\nu_a(Si-O-C-C)$), and 965 cm^{-1} ($\delta(H_3CO)$ and $\delta(H_3-CC)$).[12,13] This shows that only a partial hydrolysis of the alkoxy groups is achieved in the as-deposited films (25 °C). In the same region are observed bands at 1120 cm^{-1} $\nu_{as}(Si-O-Si)$,[14] and at 1200 cm^{-1} ($Si-CH_2-$), and 1045 cm^{-1} ($Si-CH_2-$). The 1168 cm^{-1} band, $\delta(CH_3)$, is very intense and observed as a distinct peak in the absorption spectrum; it can be used to monitor the condensation process during thermal curing. Around 120 °C a decrease in intensity is observed, and after thermal curing at 180 °C this vibrational mode is detected only as a weak shoulder. The other bands assigned to vibrations of unreacted TEOS also follow a similar trend, although their lower intensity makes it harder to follow their variations during the thermal curing. At 2844 cm^{-1} there is another absorption band that is correlated to the presence of unreacted species. This vibrational mode is attributed to $\nu_s(CH_3)$ in Si−OR (R═CH_3, CH_3-CH_2) and because around this band there is only a weak overlapping with other absorptions, it can be used also to follow the condensation with the temperature (Figure 4). The evolution of

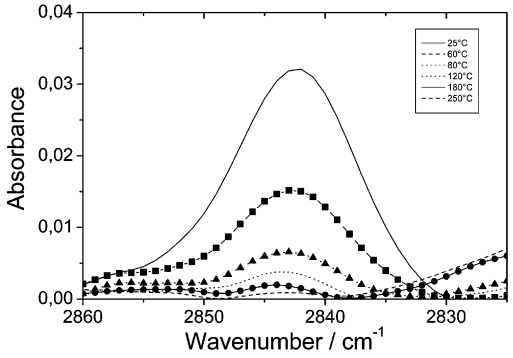

Figure 4. Changes in the 2844 cm^{-1} absorption band, $\nu_s(CH_3)$ in Si−OR, as a function of the thermal treatment temperature.

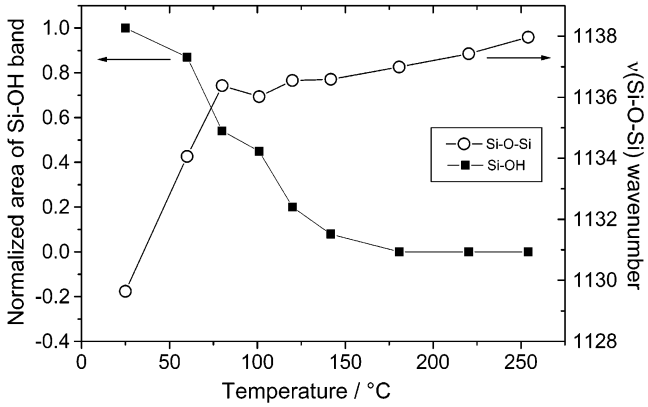

Figure 5. Normalized area of Si−OH stretching band as a function of the temperature (left *y* axis) and change of the ν_{as}-(Si−O−Si) band as a function of position of the temperature (right *y* axis).

the Si−OR bands in Figure 3 suggests that most of the condensation occurs before 120 °C. At 180−250 °C the inorganic side of the material is practically fully condensed. The results indicate that thermal curing between 120 and 180 °C causes the condensation of most of the unreacted species.

The formation of a connected silica backbone is accomplished not only through the reaction of Si−OR groups but also via the condensation of silanols, as shown by variation of the Si−OH absorption band (∼940 cm^{-1})[15,16] that decreases during thermal curing up to 180 °C when it is no longer detected. Figure 5 shows the silanols condensation as a function of the temperature together with the position of the Si−O−Si vibrational mode (Si−O−Si antisymmetric stretching). The condensation reactions are accompanied by the strengthening of the siloxane network, as revealed by the shift of the Si−O−Si absorption band to larger wavenumbers.[17−19] The effect of thermal curing on the condensation was also studied by employing ^{29}Si solid-state NMR. The analysis was performed on powders heated at 60 °C because it is quite difficult to reproduce the as-deposited film conditions. The spectrum displayed in Figure 6 shows that at this heating stage T_2 (−63 ppm), T_3 (−67 ppm) units (from APTS and MPTMS) and Q_3 (−118 ppm) and Q_4 (−110 ppm) units (from TEOS)

(11) Hayamizu, K.; Yanagisawa, M.; Yamamoto, O. *Integrated Spectral Data Base System for Organic Compounds*; National Institute of Advanced Industrial Science and Technology Tsukuba: Ibaraki, Japan, 2001 (SDBS No 6845).

(12) Kennedy, J. D.; McFarlane, W. In *Multinuclear NMR*; Mason, J., Ed.; Plenum Press: New York, 1987; p 317.

(13) Georgi, U.; Gorz, H.; Roewer, G. *Main Group Met. Chem.* **2000**, *23*, 421.

(14) (a) Brinker, C. J.; Frye, G. C.; Hurd, A. J.; Ashley, C. S. *Thin Solid Films* **1991**, *201*, 97. (b) Nishida, F.; McKiernan, J. M.; Dunn, B.; Zink, J. I.; Brinker, C. J.; Hurd, A. J. *J. Am. Ceram. Soc.* **1995**, *78*, 1640. (c) Huang, M. H.; Soyez, H. M.; Dunn, B. S.; Zink, J. I. *Chem. Mater.* **2000**, *12*, 231.

(15) Matos M. C.; Ilharco L. M.; Almeida, R. M. *J. Non-Cryst. Solids* **1992**, *147&148*, 232.

(16) Primeau, N.; Vautey, C.; Langlet, M. *Thin Solid Films* **1997**, *310*, 47.

(17) Galeener, F. L. *Phys. Rev. B* **1979**, *19*, 4292.

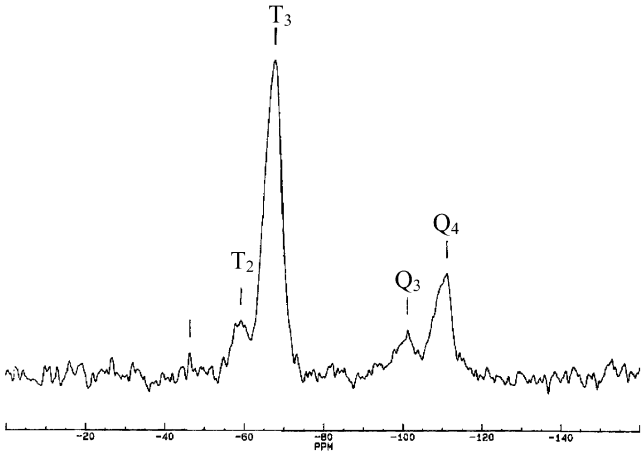

Figure 6. ^{29}Si solid-state NMR spectrum of MTA2.33-0.07-2 powders dried at 60 °C.

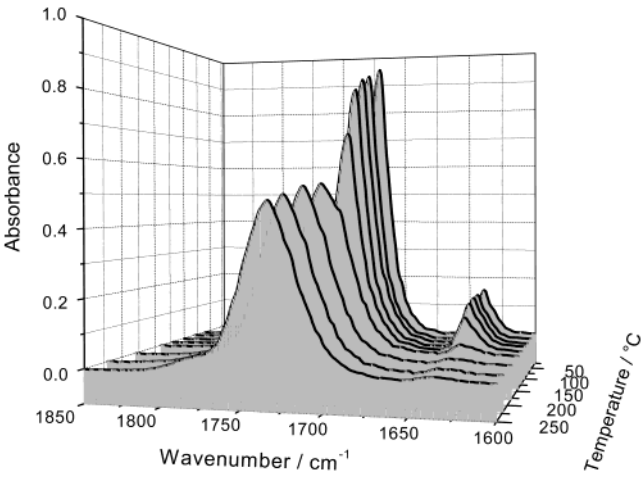

Figure 7. 3D image of the FTIR absorption spectra in the range 1850−1600 cm^{-1} of MTA2.33-0.07-2 films thermally cured at different temperatures.

are present. This finding is in good agreement with FTIR data for films (Figures 3, 4, and 5) that show that most of the condensation reactions occur during the first drying stage at 60 °C.

Thermal curing is expected to lead to condensation of the inorganic network while inducing the formation of an interconnected organic polymer via thermal opening of the C═C double bond in MPTMS.

Figure 7 shows the FTIR absorption spectra of MTA2.33-0.07-2 films as a function of the curing temperature. The spectra show two absorption bands, at 1630 and 1750 cm^{-1} assigned to C═C and C═O vibrational modes, respectively. A sudden decrease in intensity of the former band is observed between 100 and 150 °C, indicating that the organic polymerization occurs within this range of thermal curing temperatures. This change in the 1630 cm^{-1} band is simultaneously accompanied by a decrease in intensity and broadening of the C═O band, due to the loss of conjugation with C═C with the increase of the polymerization.

After thermal curing at 180 °C, up to a 98% degree of polymerization (which is calculated by the variation of the area attributed to the vibration of C═C bonds) is achieved, as shown in Figure 8 where the degree of polymerization as a function of curing temperature is reported. The polymerization was not affected by the

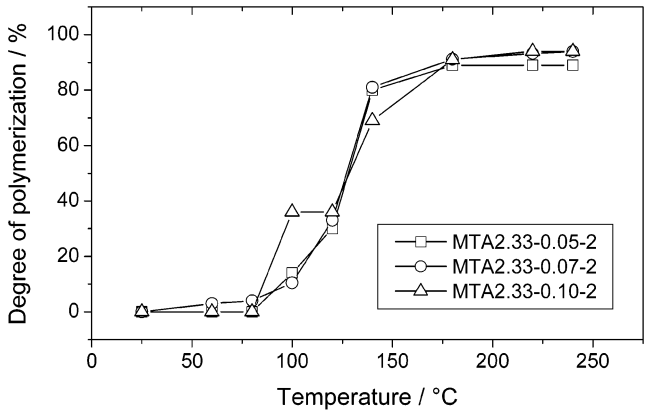

Figure 8. Degree of polymerization of thermally cured MTA2.33-0.07-2 films plotted vs the temperature of curing.

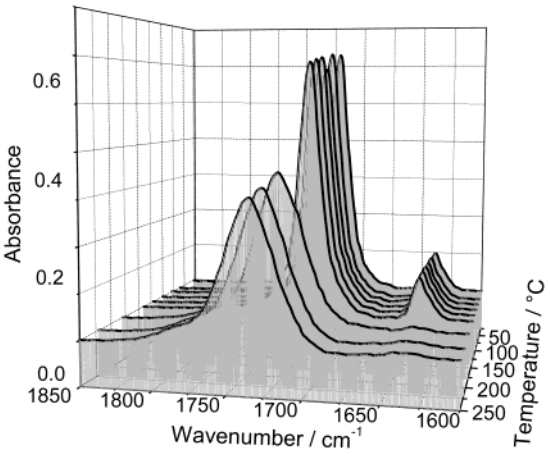

Figure 9. 3D image of the FTIR absorption spectra in the range 1850−1600 cm^{-1} of MTA1-0.07-2 films thermally cured at different temperatures.

amount of amine introduced in the precursor sol; in fact, the curves related to samples prepared with different amounts of APTS are overlapping. Variations in the APTS content cause, however, differences in the gelation time of the sols. The data reported in Table 1 show that lower amounts of APTS produce longer gelation times.

The change in the H_2O/TEOS ratio from 2 to 3 did not affect the structure of the films, according to FTIR spectra (not shown in Figures). Outside this range of values, i.e., lower than 2 and greater than 3, the sols became immediately opaque upon addition of APTS and could not be used for the preparation of optically transparent films. A decrease in the MPTMS/TEOS ratio (1 instead of 2.33) affects the film structure mainly with respect to the organic polymerization. No significant variation in the IR absorptions due to the inorganic network were observed (not shown in Figures).

The larger amount of TEOS in the precursor sol will produce a hybrid organic−inorganic network with a more extended silica backbone and will affect the organic polymerization process. Figure 9 shows the FTIR absorption spectra of MTA1-0.07-2 films cured at different temperatures; it is interesting to observe that, with respect to the samples containing a larger amount of APTS, the beginning of polymerization is delayed to higher temperatures, around 180°C. The films with the larger amount of APTS (MTA1-0.10-2), however, polymerize at a lower temperature, as observed in Figure

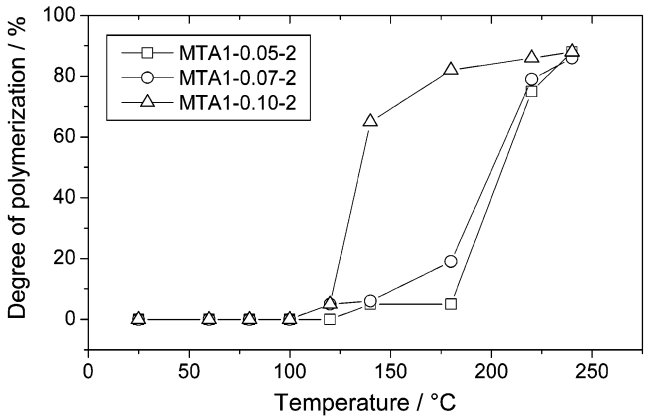

Figure 10. Degree of polymerization of thermally cured MTA1-0.07-2 films plotted vs the temperature of curing.

10, where the degree of polymerization as a function of the temperature is reported for films derived from syntheses carried out with different APTS amounts. This behavior is explained by the fact that in polymerizable hybrid materials formation of the inorganic and organic networks is a competitive process. If the growth of the organic chains happens when the inorganic network is already completely formed, the mobility of the organic groups is dramatically hindered and there is not enough free space in this already rigid framework to reach a large degree of polymerization. APTS is a "weak" basic catalyst, but it is also a network modifier that will decrease the degree of condensation of the overall network, bringing some flexibility, and facilitating the growth of organic chains.

In the present conditions, therefore, thermal curing of the films produces an almost simultaneous condensation of the silica network and the opening of C═C double bonds. At 180 °C a 98% degree of polymerization is reached (Figure 8). This very large efficiency of the process can be obtained if the extent of condensation of the inorganic backbone is not sufficient enough to hinder the growth of the organic chains. The simultaneous growth of the two networks between 50 and 150 °C enables reaching this efficient polymerization.

To evaluate the conversion of acrylate double bonds, we have monitored the changes in intensity of the ν(C═C) absorption band at ∼1640 cm^{-1} and ν(C═O) vibration at ∼1720 cm^{-1} with the thermal treatment. Figure 11 shows the FTIR absorption spectra in the range 1800−1650 cm^{-1} of MTA2.33-0.07-2 films cured at 25 °C (Figure 11(a)) and 140 °C (Figure 11(b)). The spectra were simulated using three Gaussian components that are labeled 1, 2, and 3 in Figure 11. Band 3 (∼1700 cm^{-1}) is assigned to carbonyl groups which are hydrogen-bonded to silanols,[20] and this mode is only weakly detected in the 140 °C cured films. Component 2 is assigned to C═O stretching vibrations that are conjugated to C═C double bonds. This is the main component in the 25 °C films before curing. Component 1 is assigned to the vibrations of C═O groups located in a more cross-linked microstructure as revealed by the shift to larger wavenumbers, the broadening, and

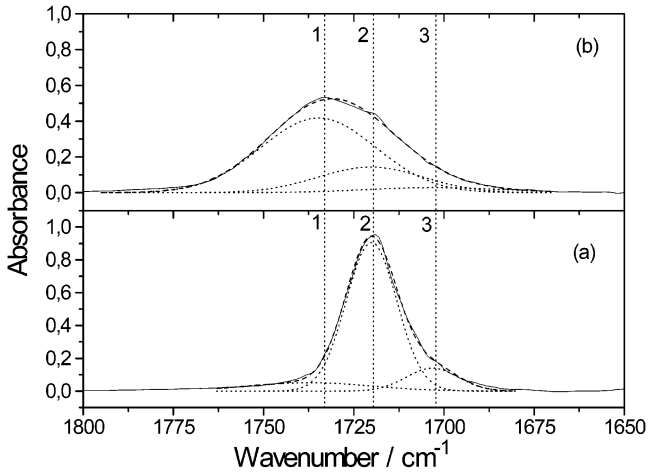

Figure 11. Deconvolution of the FTIR absorption spectra of MTA2.33-0.07-2 films cured at 25 °C (a) and 140 °C (b).

decrease in intensity of the band. Bands 1 and 2 are, therefore, correlated to the same C═O mode but in two locally different structural environments. The ratio between the areas of bands 1 and 2 in Figure 11(b), which are related to samples fired at 140 °C, shows that there is a 25% difference in the two areas, which is very close to the value calculated from the intensity of the 1640 cm^{-1} band (Figure 8). This observation supports the present attribution, suggesting that the signals 1 and 2 can be used to get a qualitative evaluation of the polymerization. It should be observed also that the polymerization, which restricts the C═O mobility, is due to the growth and/or condensation of the organic and inorganic networks, which at 140 °C reach an almost simultaneously large extension. (Figures 3, 5, and 8).

Multinuclear Solid-State NMR Study of Powdered Samples. Three powdered samples thermally cured at different temperatures were analyzed using solid-state NMR. ^{13}C CP MAS solid-state NMR was used to investigate in more detail the polymerization process induced by thermal curing. Even though the NMR data are recorded on powdered samples of the same composition as the films (MTA2.33-0.07-2) they should be compared with some caution because of the differences due to their preparation; they can, however, give direct and complementary information about the organic polymerization process. Figure 12 shows the ^{13}C CP MAS spectra of MTA2.33-0.07-2 samples after thermal curing at 60, 120, and 250 °C. Assignments of MPTMS ^{13}C signals before and after the thermal polymerization are reported in Table 2. Signals located at 125 and 137 ppm correspond to carbons of the C═C groups. They decrease in intensity at 120 °C and disappear by 250 °C. The resonance peaks due to the C═O groups show similar behavior. At 120 °C, a new peak appears at 177 ppm, besides the main signal at 168 ppm, due to polymerization reactions which change the local environment of the C atoms that were close to the C═C bonds (Scheme 1). The coexistence of two C═O groups was also observed in the FTIR spectra (Figure 11). At 250 °C the initial signal at 167 ppm has disappeared, and the new signal is enclosed (see Scheme 1) and/or broadened indicating a low mobility of the C═O groups or a distribution of chemical shifts. The formation of an organic polymer at 250 °C is also supported by the presence of a new signal at 45 ppm, which is attributed

(18) Almeida, R. M.; Pantano, C. G. *J. Appl. Phys.* **1990**, *68*, 4225.
(19) (a) Almeida, R. M.; Pantano, C. G. *J. Appl. Phys.* **1990**, *68*, 4225. (b) Innocenzi, P. *J. Non-Cryst. Solids* **2003**, *316*, 309.
(20) Li, X.; King, T. A. *J. Non-Cryst. Solids* **1996**, *204*, 235.

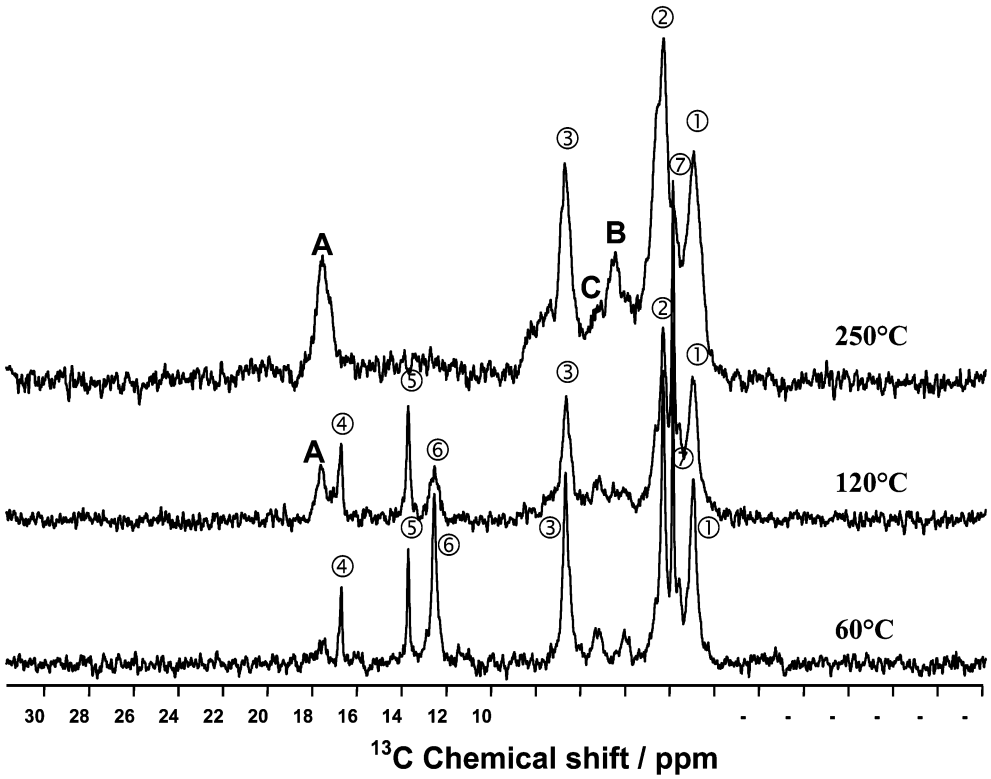

Figure 12. ^{13}C CP MAS NMR spectra of MTA2.33-0.07-2 samples thermally cured at 60, 120, and 250 °C (from the bottom).

Scheme 1

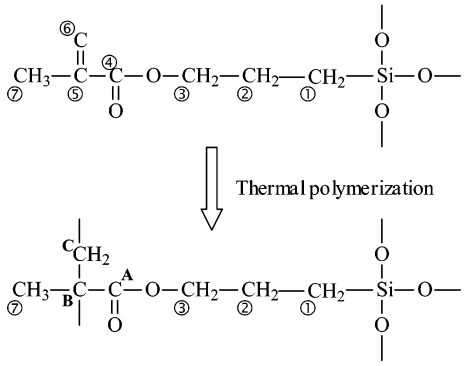

to tetrasubstituted $C^{⑤/B}$ (Scheme 1). The broadening with thermal curing can be observed with all the resonance peaks—not only those involved in the organic polymerization. The important broadening of the peak at 9 ppm, due to the first carbon close to the silicon in MPTMS is, indeed, an indication of a loss of mobility due to the advancement of the inorganic polycondensation.

Some questions arise about the presence of a resonance peak of weak intensity around 40 ppm, which is clearly detected at 60 and 120 °C (Figure 12) and likely overlapping at 250 °C with the signal due to the quaternary carbon. To assign these signals, we have assumed a possible reaction between MPTMS and APTS (Scheme 2), which should give rise to a new signal at 40 ppm, together with another signal at 55 ppm, that could overlap the resonance peak of the $-CH_2-$ carbons in the polymerized MPTMS. Different experiments, performed with much larger APTS contents with respect to MPTMS have shown a stronger increase of these two signals with the amount of APTS, supporting our attribution.

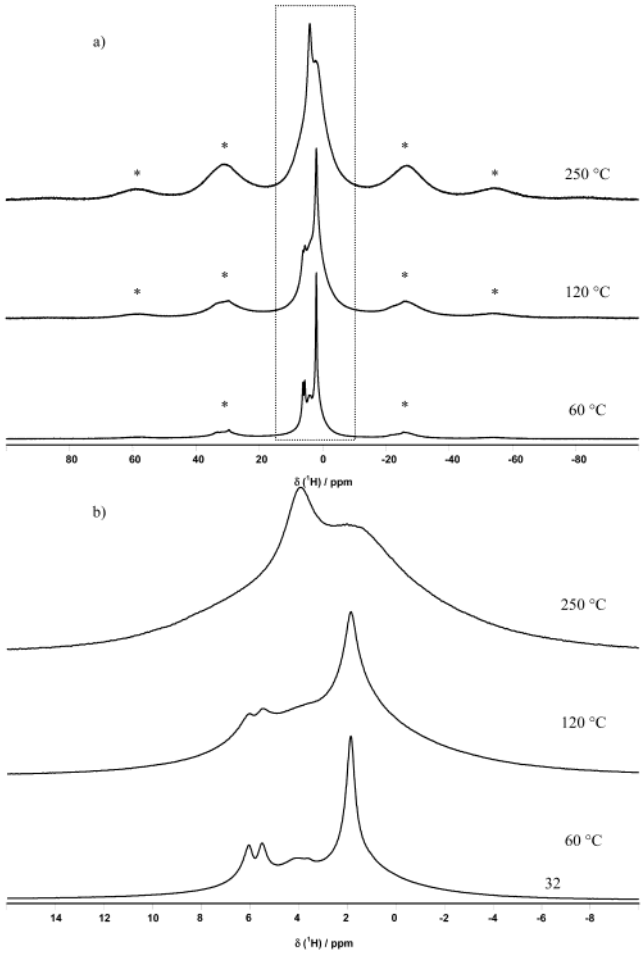

Figure 13. ^{1}H solid-state NMR spectra of MTA2.33-0.07-2 sample treated at 60, 120, and 250 °C (a), and enlargement of the 16 to −10 ppm region.

Table 2. Assignments of the Signals in the ^{13}C CP MAS NMR Spectra of the MTA2.33-0.07-2 Samples

chemical shift (ppm)	units	comments	label[a]
9	$-CH_2-\boldsymbol{C}H_2-Si\equiv$	first carbon linked to the silicon	①
22	$-\boldsymbol{C}H_2-CH_2-Si\equiv$	second carbon close to the silicon	②
67	$-O-\boldsymbol{C}H_2-CH_2-CH_2-Si\equiv$	third carbon close to the silicon	③
167	$-\boldsymbol{C}(=O)-$	carbon close to vinylic carbons, before the C=C opening	④
137	$C=\boldsymbol{C}$	vinylic carbon atom	⑤
18	$\boldsymbol{C}H_3-C-$	carbon in the methyl terminal group	⑦
126	$\boldsymbol{C}H_2=C-$	vinylic carbon atom	⑥
177	$-\boldsymbol{C}(=O)-$	carbon close to aliphatic carbons, after the C=C opening	A
45	$-(-\boldsymbol{C}-)-$	quaternary carbon	B
55	$-\boldsymbol{C}H_2-$	carbon in the polymerized hydrocarbon chain	C

[a] The numbers from 1 to 7 are used as labels for the carbons in mptms, and the letters are used for carbons in MPTMS after reaction of the C=C double bond.

Scheme 2

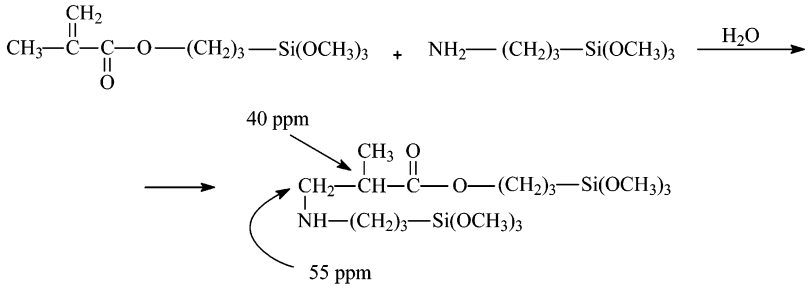

^1H MAS NMR have also been recorded on the same samples (Figure 13). At a moderate MAS rate (11 kHz), the spectra show very different spinning sideband patterns (Figure 13a). This can be related to contrasted strength in the ^1H homonuclear dipolar interaction. As no significant increase in proton density could be considered to explain this behavior, a large decrease in the mobility of the protonated species was assumed when pursuing the thermal treatments. This might be in accordance with the completion of polymerization or parallel reactions (Schemes 1 and 2). From the spectrum of the sample treated only at 60 °C, we could distinguish three regions of ^1H chemical shifts (Figure 13b). First, an intense signal located at c.a. 1.5 ppm may account for the various methyl and methylene groups attached to carbons through single bonds. We assign the additional broad signal around 4 ppm to methine attached to oxygen or to nitrogen (in this case, the amount of amine is low). The last two sharp peaks at 6.1 and 5.5 ppm correspond to the protons bonded to the C=C double bonds. Even if the loss in resolution and the increase in the spinning sideband signals do not permit following the variations in signal intensity, we observe a qualitative decrease of these last peaks that might also be associated with double bond opening.

Conclusions

Optically transparent hybrid organic−inorganic films have been prepared from 3-aminopropyltriethoxysilane, 3-methacryloxypropyltrimethoxysilane, and tetraethyl orthosilicate. NMR spectra of the sols have shown that the alkoxides are poorly condensed in solution prior to deposition. This is consistent with the characterization of the as-deposited film performed by FTIR absorption spectra showing a low extent of condensation for the solid network. Thermal curing of the films produces a simultaneous condensation of the silica network and the opening of C=C double bonds. At 180 °C, a degree of polymerization of 98% is reached. This very large efficiency of the process can be obtained because the degree of condensation of the inorganic backbone is not large enough to hinder the growth of the organic chains.

Acknowledgment. Part of this work was funded from an EEC ARI contract HPRI-CT-1999-00042. P. Innocenzi, G. Brusatin, S. Licoccia and M. L. Di Vona acknowledge MIUR (Italy) for financial support.

CM0343305